

# STAR Geometry

Howard Matis, Rene Bellwied, Gary Eppley, Detlef Irmscher, Peter Jacobs, Spencer Klein, Tom LeCompte, Mike Lisa, Iwona Sakrejda, Marguerite Tonjes, Dhammika Weerasundara, Pablo Yepes, Roy Bossingham  
STAR Note CSN229B

A general philosophy for numbering elements on the STAR detector is presented. This document describes the numbering system for the TPC, EMC, CTB/TOF, FEE and SVT. These numbers should be used to identify elements for both hardware and software.

Version 1.0 — November 21, 1995 - Document issued

Version 2.0 — March 12, 1996 - Defined EMC Barrel Geometry

Version A — September 25, 1998 - Modified CTB numbering. Made this document a controlled STAR note. Modified EMC geometry to reflect actual detector.

Version B — September 27, 1999 — Describe time bucket numbering for the TPC.

It is important to have a common numbering system for both hardware and software. By having a well-defined and consistent labeling scheme, we can avoid much confusion. This document describes the system that the STAR collaboration has adopted.

During the August 1995 STAR collaboration, representatives from STAR met and agreed upon a common geometry and numbering system for both hardware and software. The note describes what is now the official STAR geometry and numbering scheme. All future drawings, labels and programs should follow the conventions established by this note.

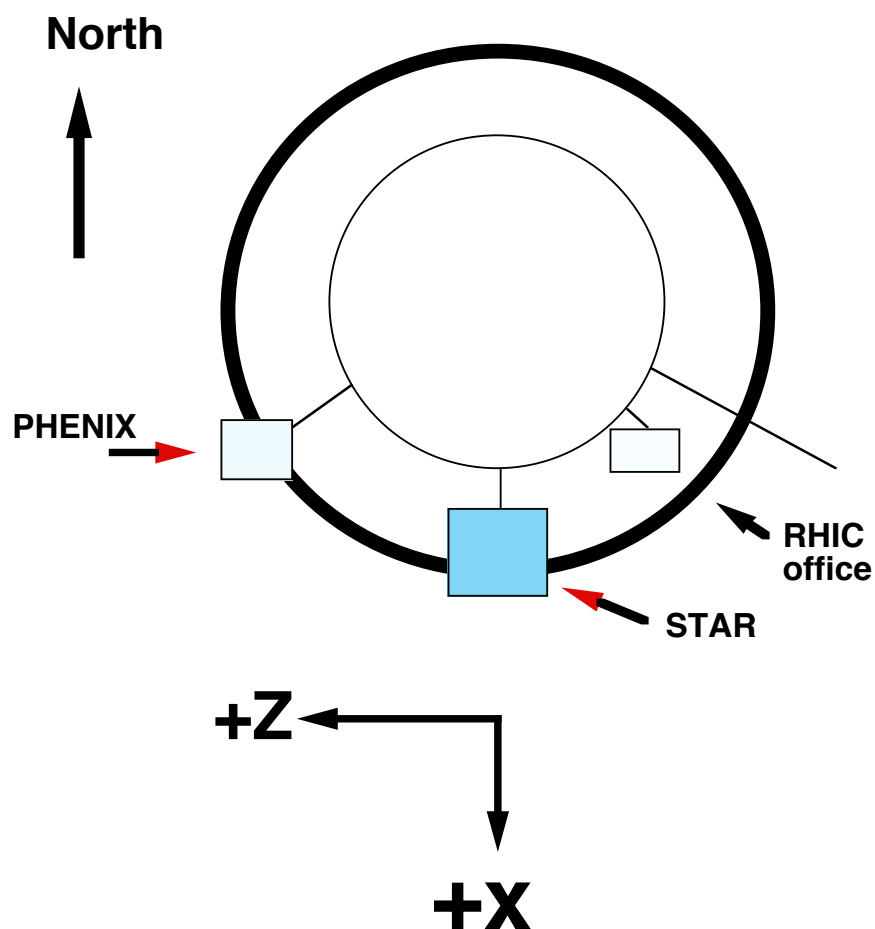


Figure 1: STAR coordinate system shown in relationship to RHIC. The STAR geometry is described in STAR note #121. Figure 1 shows a picture of RHIC looking from above the accelerator. As stated in SN #121, the standard STAR coordinate system is defined by:

- Positive y is up.
- The origin of the coordinate system is located at the center of the solenoid (iron). The direction y is perpendicular to the axis of the solenoid. The y-z plane is vertical and positive y points opposite (as closely as possible) the direction of gravity.
- Positive x points approximately south and away from center of the RHIC accelerator. Positive z points westward.
- The direction of the RHIC beam is defined by a view looking down upon the accelerator. At our detector the clockwise beam travels toward positive z and the counter-clockwise beam moves toward negative z.

### **General STAR Policy for Geometry**

All detectors should be first numbered from the +z side (West End) looking toward the interaction region. The geometry of the detector is defined by the layout of the TPC wheel. If a detector needs additional number for detectors on the -z side, then the numbers should be consecutive with the +z elements.

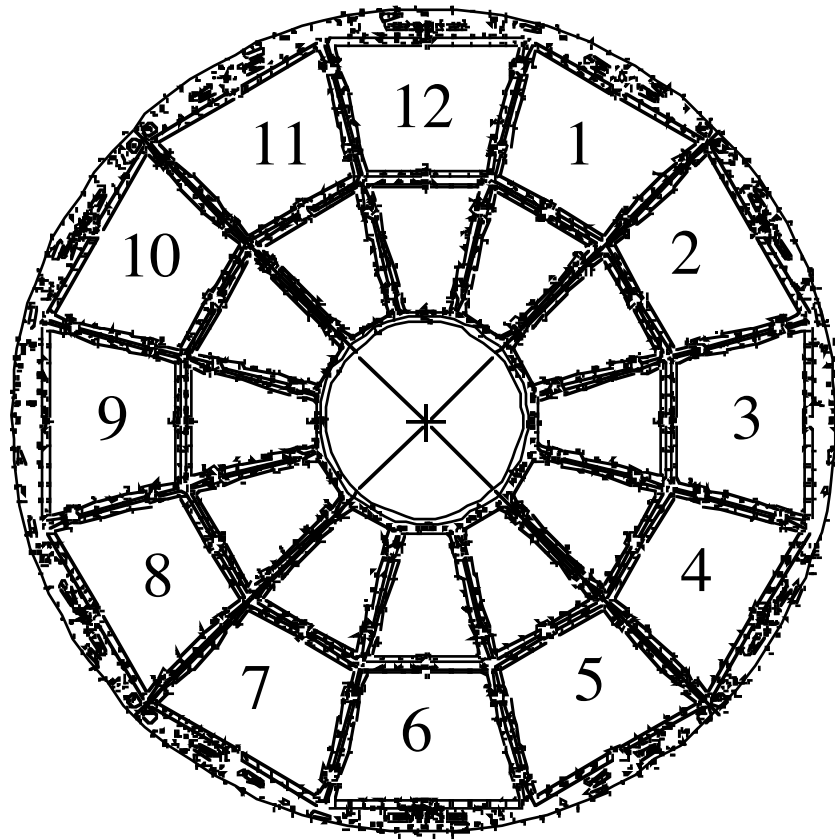


Figure 2: Aluminum frame for the TPC wheel.

### **TPC geometry and numbering scheme**

The TPC sectors are numbered according to the STAR specification. The numbering is similar to that of a clock. The +z sectors are numbered from 1-12 while the -z sectors are numbered from 13-24. Each sector is numbered clockwise from the perspective a person looking into the TPC.

From a perspective of a viewer (facing east) outside of the detector, Figure 3 shows from the numbering for the West Side sectors ( $z > 0$ ).

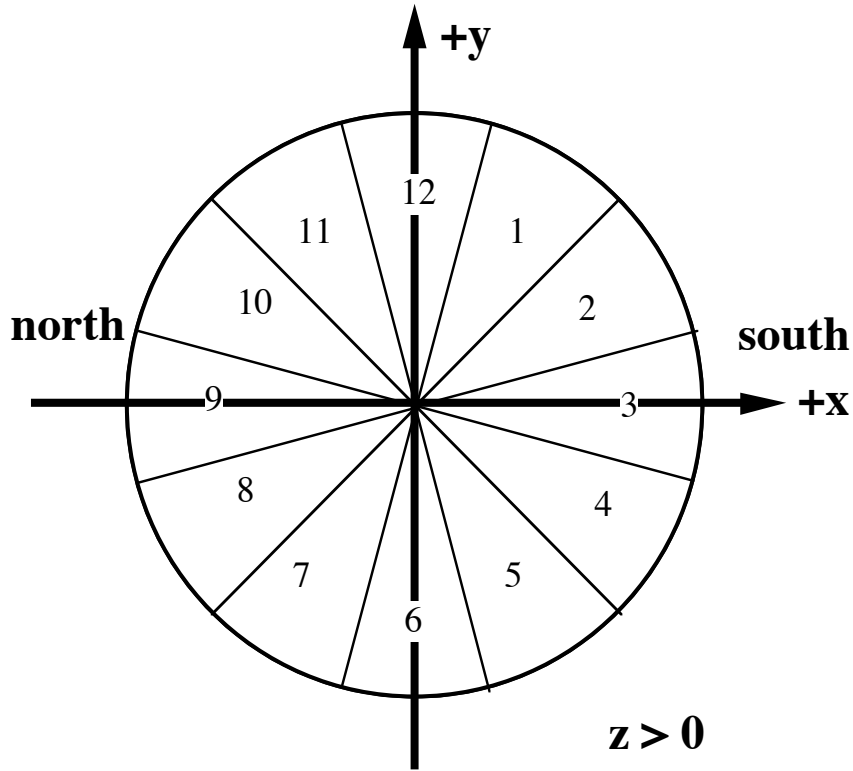


Figure 3: This is the West End of the detector when one is looking from the outside.

Again looking from the outside of the detector, the East Side ( $z < 0$  side) starts with TPC sector number 13. The numbering is pictured in Figure 4.

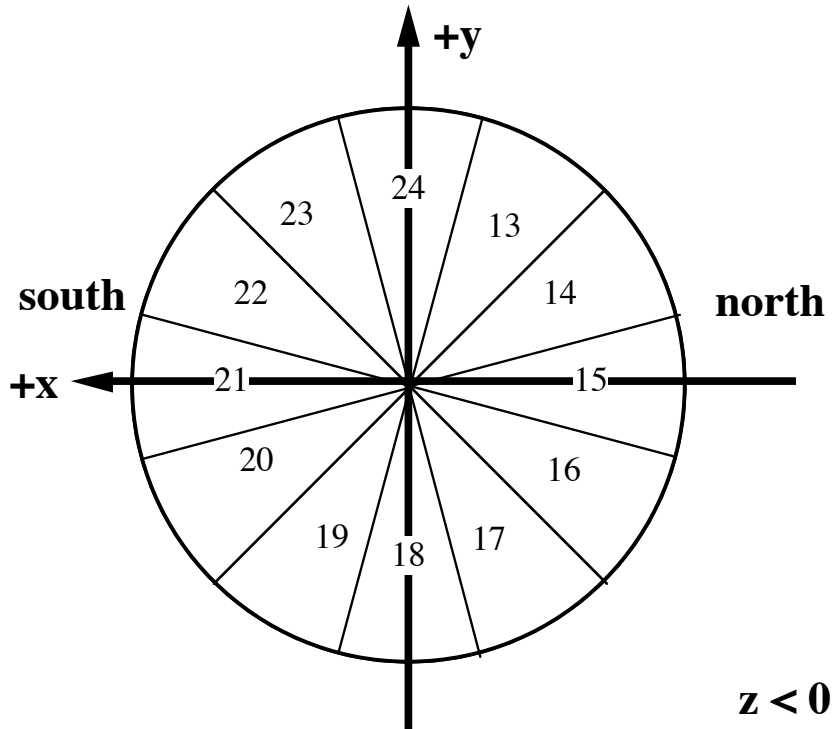


Figure 4: This is the East End view of the detector when one is looking at the endcap from the outside.

Note that there is no division between labels for the outer and inner sectors. The arrows in Figures 4 and 5 indicate the x- and y-axis.

A consequence of this numbering scheme is that a particle traveling parallel to the beam from sector 2 enters sector 22 on the other side of the central membrane. While there is a slight break in symmetry, the endcap numbering as seen from the outside is much simpler for installing hardware on the detector.

We number the pads using the following algorithm:

- **Pad row numbering**—the pad rows are numbered 1 to 45 starting from inside. Pad row  $n$  indicates the center of the  $n$ -th pad row.
- **Pad numbering**—the pads in each pad row are numbered from left to right looking from the outside of the TPC starting. Pad 1 is the first pad. The location of Pad  $n$  is the center of the  $n$ -th pad.

### **CTB/TOF Geometry**

The CTB trays are numbered with two indexes corresponding to their azimuth angle,  $\phi$ , and their  $z$  coordinate. CTB trays are numbered from 1-60 on the  $+z$  half of the detector (clockwise from the perspective of a person facing the center of the detector from the  $+z$  side). On the  $-z$  side, the trays are numbered from 61-120 (clockwise from the perspective of a person facing the center of the detector from the  $-z$  side). The CTB slats are numbered from 1 to 2 in each tray starting with the inner slat. Slat 1 is located from  $0 < |\eta| < 0.5$  while slat 2 is located from  $0.5 < |\eta| < 0.97$ .

Figure 5 shows the numbering criteria for the CTB trays ( $\phi$  direction) inserted on the West Side. Figure 6 shows the numbering criteria for the slats within a tray ( $\eta$  or  $z$  direction), while Figure 7 shows the numbering criteria ( $\phi$  direction) for trays inserted on the East Side. TOF trays will be numbered the same way but will have more slats in  $\eta$  and will have more subdivision in  $\phi$ .

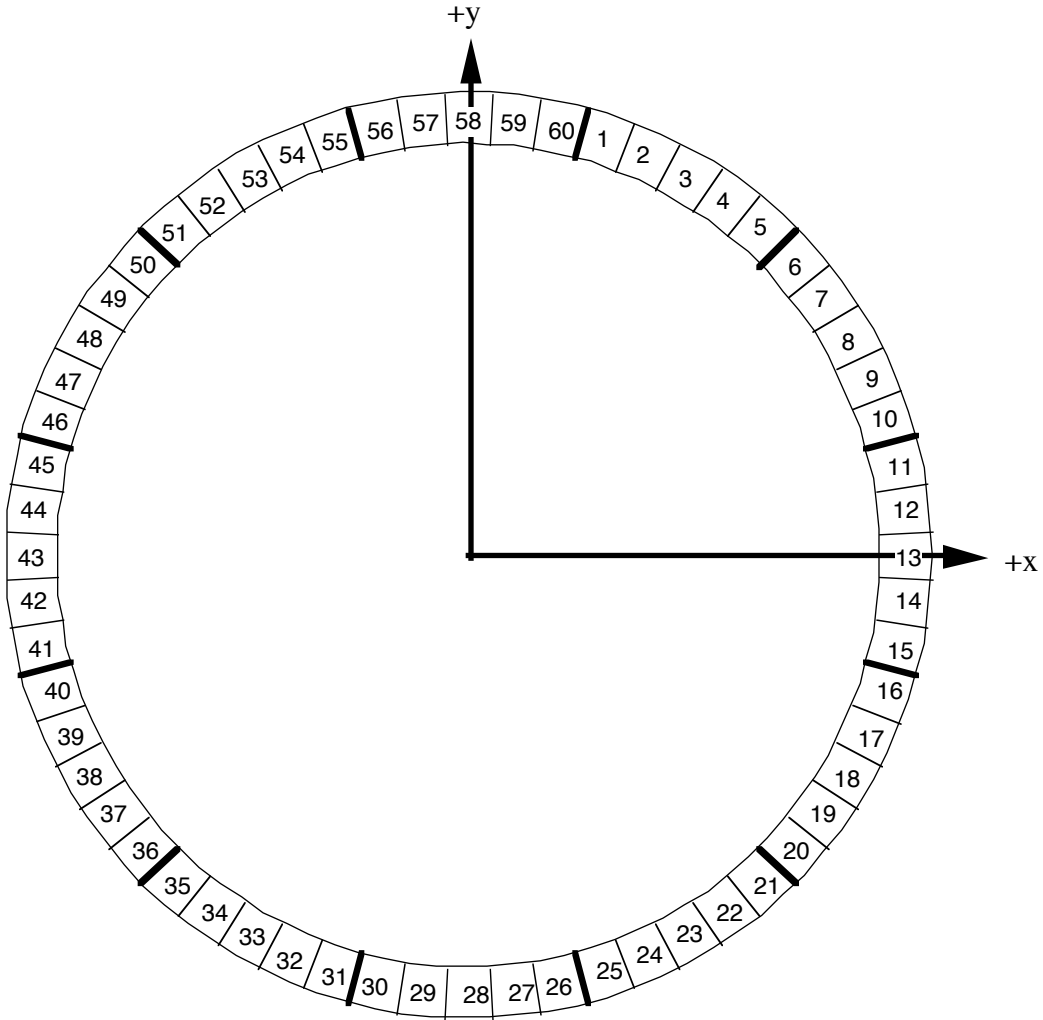


Figure 5: Numbering of the CTB modules in phi for  $z > 0$ . Note that the heavy line between the modules indicates the boundaries of the TPC sector by which they are supported.

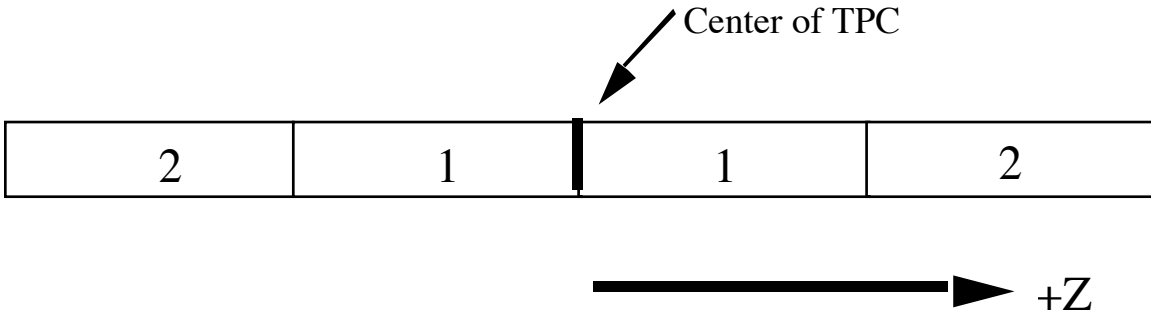


Figure 6: Numbering of the CTB modules in z. Note that the heavy indicates the center of the TPC. Each CTB tray holds two modules.

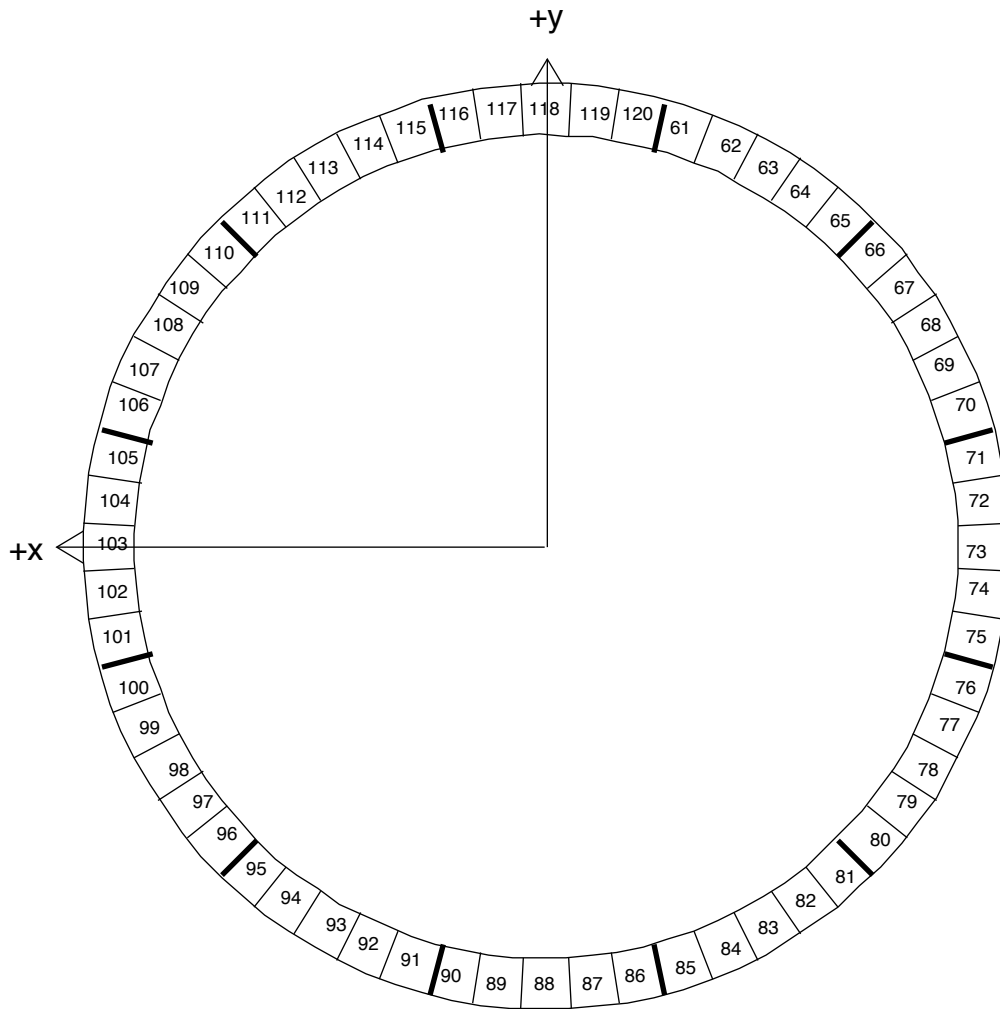
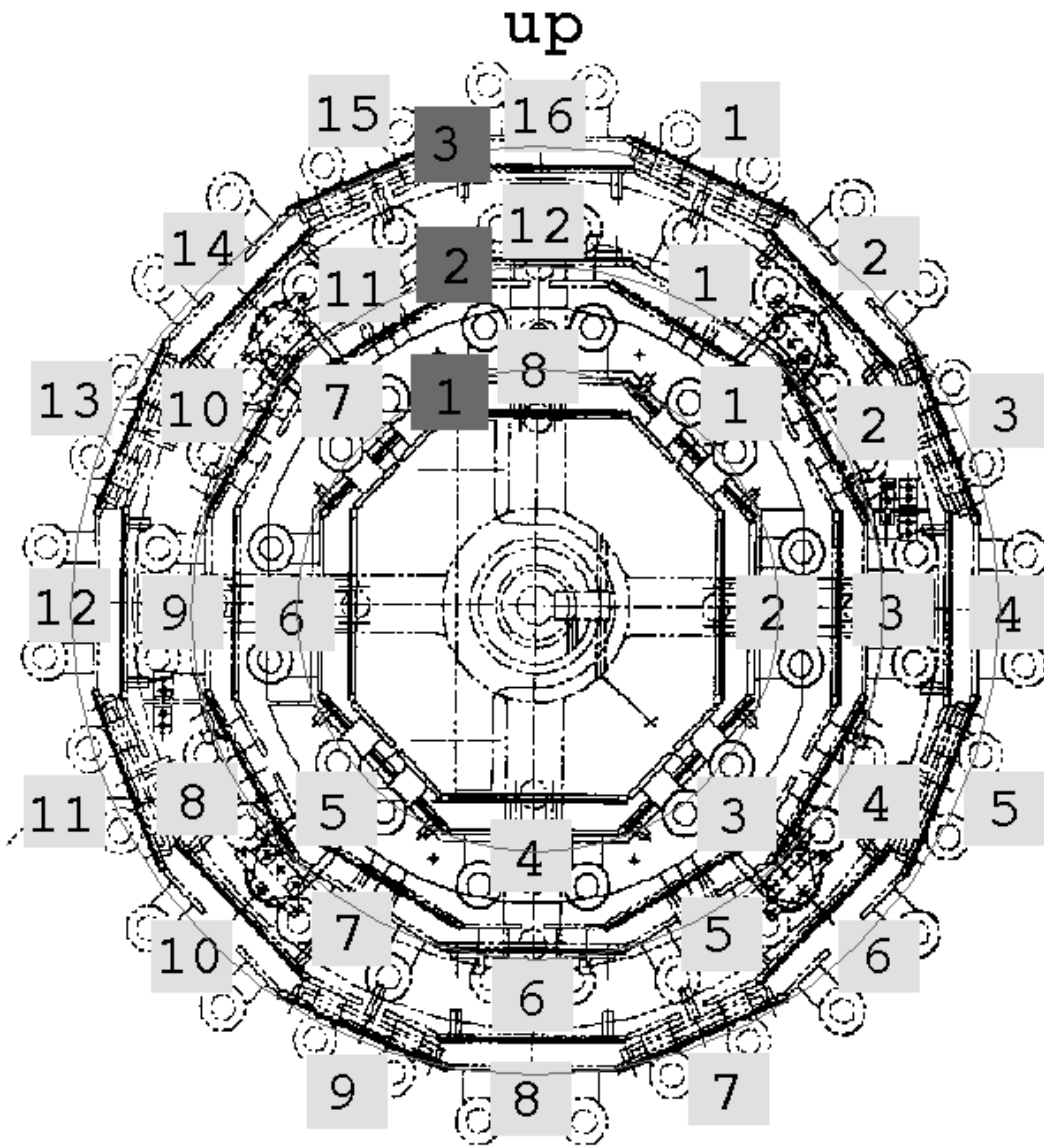


Figure 7: Numbering of the CTB modules in phi for  $z < 0$ . Note that the heavy line between the modules indicates the boundaries of the TPC sector by which they are supported

### SVT Geometry

The SVT is numbered in a similar way as the rest of the detectors. Since the ladders are continuous along the beam axis, they are only numbered from the +z side. However, the ladders do not align with the TPC sector boundaries. Therefore, we define the last ladder in a barrel as the one which is vertical and on top. The first ladder starts clockwise. For instance in Figure 8, the light shaded numbers indicate the ladder number. The dark shaded numbers indicate the barrel identification number. From this diagram, it is easy to see that barrel 1 goes from 1-8, ladder 2 from 1-12 and ladder 3 from 1-16.



**View of the SVT from the west**

Figure 8: Ladder numbering for the SVT. The dark shaded numbers indicate the barrel number, while the light shaded numbers indicate the ladder number.



The wafers on each ladder are numbered from -z to +z. Figure 9 shows the numbering scheme.

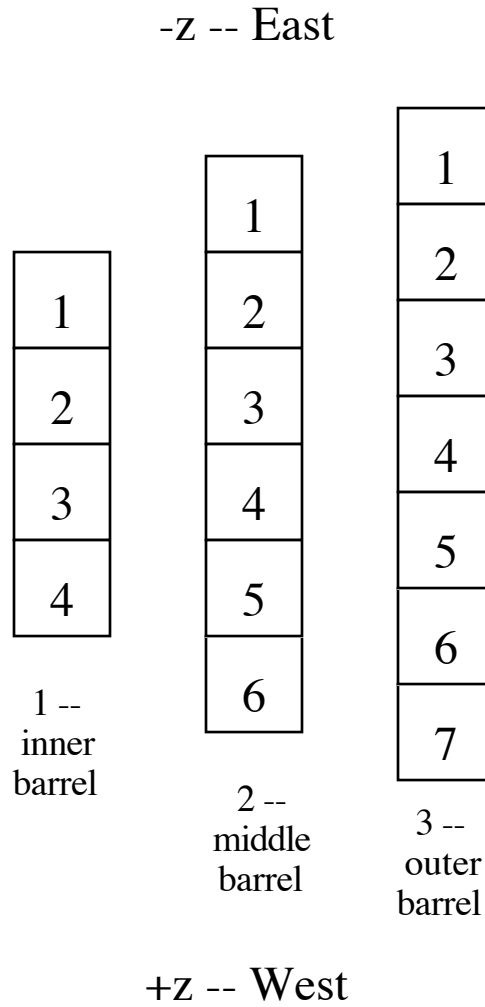


Figure 9: Numbering scheme for the wafers on the SVT ladder.

Each wafer has two hybrids. The hybrids are number clockwise when looking from the West End or left to right when looking above the barrel. (The beam axis is below the wafer.) Figure 10 shows the labeling.

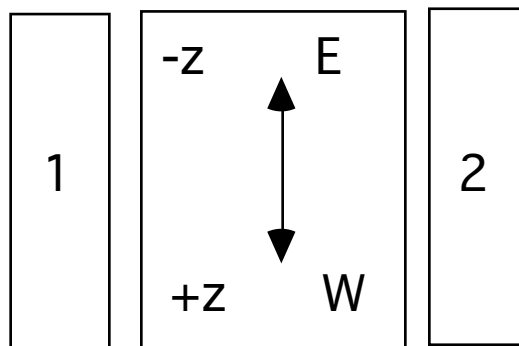


Figure 10: Labeling of a hybrid on a wafer. This is a top view with the axis of the beam line below the wafer.

## TPC FEE Geometry

Each supersector of the TPC contains 6 readout boards (RDO), which read out 181 Front End Electronic (FEE) cards. The FEE cards contain the pre-amp, shaper, and digitizer circuits while the RDO boards multiplex the data to a single fiber that then goes to the DAQ electronics.

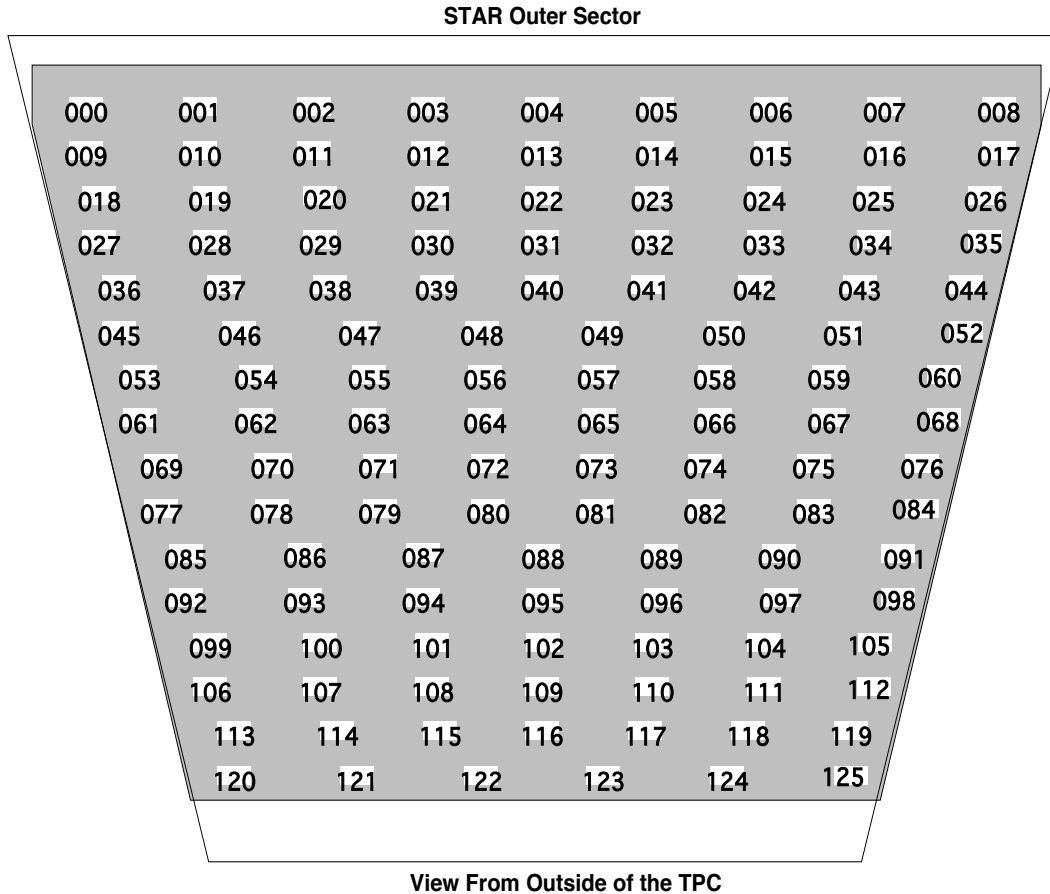


Figure 11: Outer sector of the TPC. The locations and numbers of the FEE boards are shown.

The 8 bit FEE card id numbers, which provide a cabling geographical identification, are etched onto the TPC pad plane. This information can be read out in the normal data stream. The FEE cards on the outer sectors are labeled from 0 to 125 while the cards in the inner sector are labeled from 127 to 181 (126 is missing). Card # 0 is in the outer left (looking from the outside of the TPC) hand corner of the sector as shown in Figure 11. Figure 12 shows the inner sector. This numbering scheme is contrary to the current STAR philosophy of starting with the inner sector and numbering from the center of the detector. However, the numbers cannot be changed as the hardware was built before this note was issued.

The 512 time samples from each FEE-instrumented pad or wire are assigned ID's from 0 to 511, starting from earlier times and counting upwards toward later times. Either end of the range may be truncated before data is output by DAQ, so the range of observed sample numbers may be less—even for so-called "black" data.

Since ionization electrons drift towards the pad plane, signal samples corresponding to ionization originating close to the central membrane have larger ID numbers than those corresponding to ionization originating closer to the pad plane at which the samples were recorded.

The TPC FEE ADC's synchronously sample the signal close to the trailing edge of the ADC sampling clock pulse (with the trailing edge corresponding to ionization originating further from the pad plane). However, due to various time delays, the absolute time offset of the ADC samples varies from channel to channel. In addition, the period of the ADC sampling clock can be varied from run to run. Therefore, the Z position assigned to a given ADC sample is, in general, both time- and position-dependent.

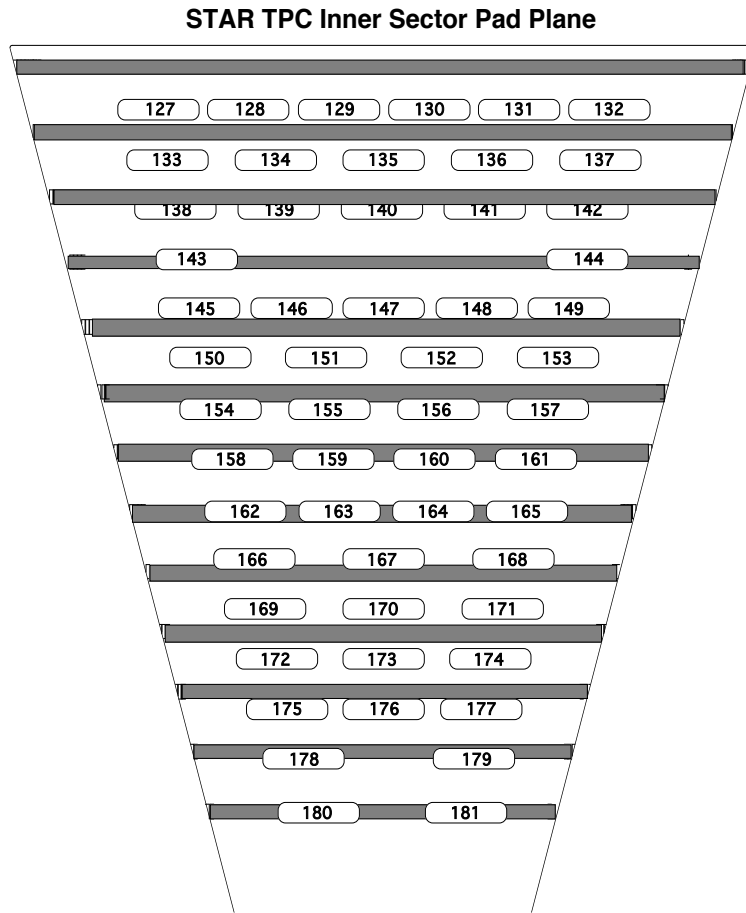


Figure 12: Representation of an inner sector of the TPC. The numbering of the FEE cards is shown.

The readout boards have addresses ranging from 1 to 6, with 1 being the innermost board and 6 the outermost. Figure 13 shows a representation of the RDO layout. The addresses of the board are determined by connectors attached to the TPC pad plane. This id provides the same geographic address test capacity as the FEE boards. Also, these addresses are used in the sector HDLC networks. There are two RDO boards (1-2) on the inner sector and four (3-6) on the outer sector.

Further details on the FEE electronics and on the order of data readout are given in "Front End Electronics <-> DAQ Receiver Board Fiber Optics Interface Specification, V. Lindenstruth et al. This document can be presently found in the STAR WWW pages. To

find the document, go to the STAR “group page” and look under “Interfaces.” As of the date of this note, 1.a is the most recent edition. However, 1.a contains a slightly different numbering scheme and a rotated TPC wheel. Work is in progress on an update. Please note that some older mechanical drawings have used a different numbering scheme.

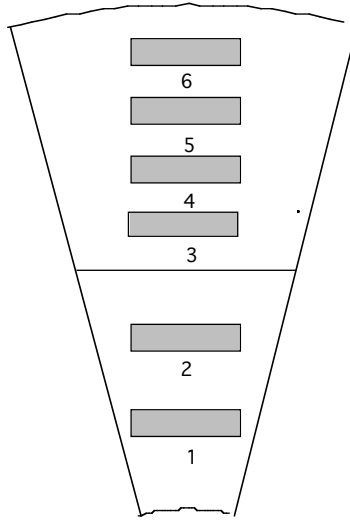
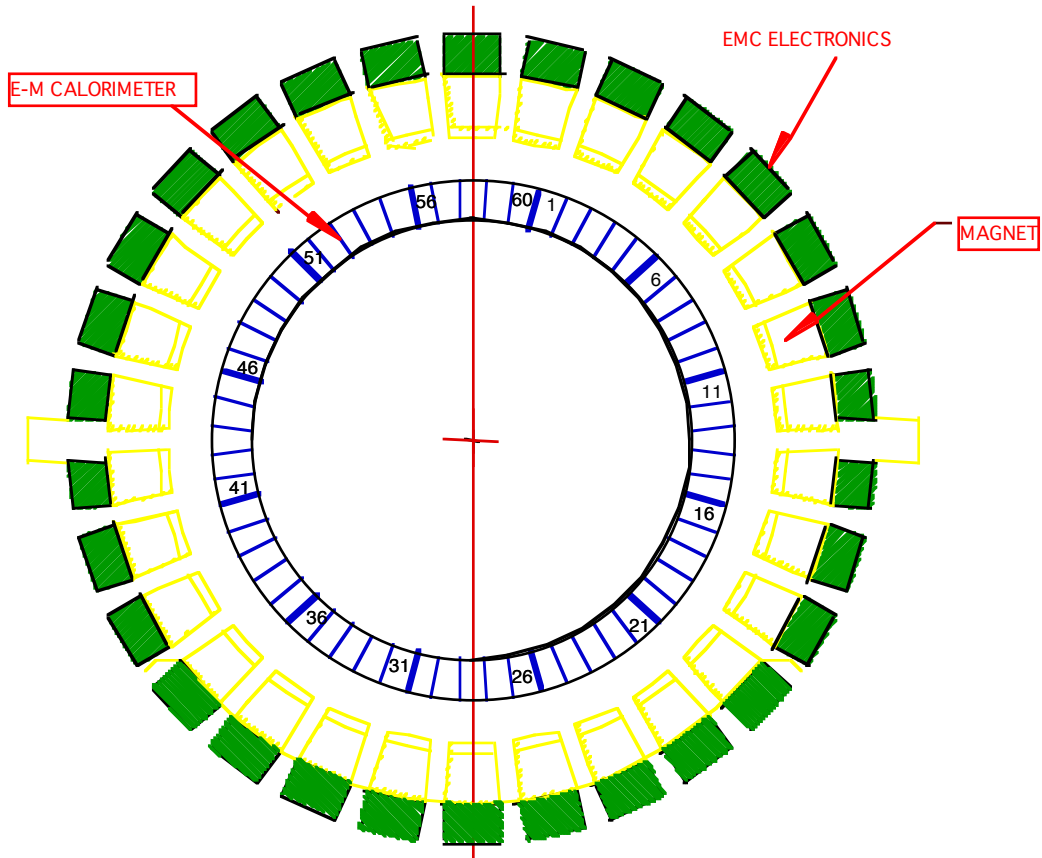


Figure 13: Schematic that shows the numbering of the RDO boards. This drawing is not to scale.

### **EMC Barrel Geometry**

The full implementation of the EMC Barrel consists of 120 **modules**. There are 60

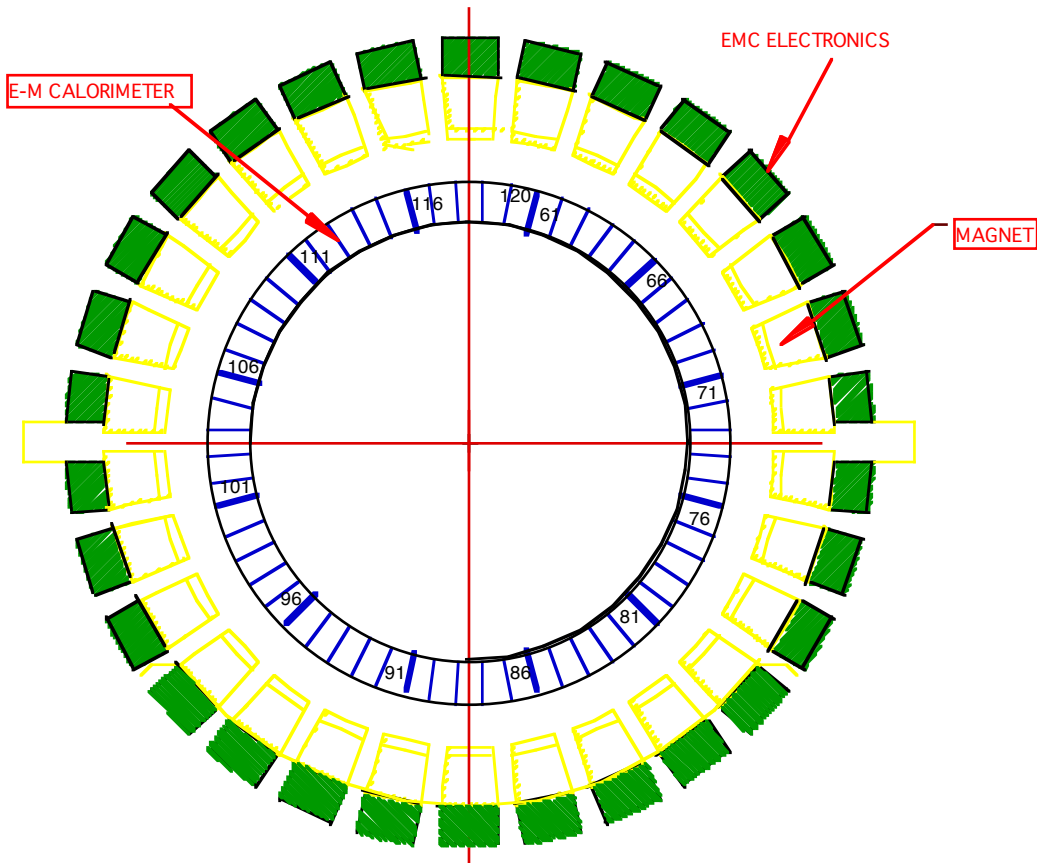


## EMC as seen from +z

Figure 14: EMC detector viewed from the outside while looking toward the interaction point.

modules in +z and 60 modules in -z. Each module has 20 **towers** in the z direction and 2 towers in the  $\phi$  direction. There is no more segmentation, although the first two layers (closest to the interaction point) contain the pre-shower information. In addition, each module has a **shower max** detector. When the EMC End Cap Calorimeter design becomes more refined, its geometry will be included in this note.

The azimuthal boundaries of the EMC modules are aligned with the CTB/TOF elements and the TPC sectors. The azimuthal numbering for the EMC is the same as for the CTB/TOF modules. The -z modules are numbered from 61-120 beginning at the boundary between TPC sectors 13 and 24, and increasing clockwise when viewing the detector from the -z end. On the +z side, the top two modules are numbered +58 (over TPC sector 12) and number 118 (over TPC sector 24). Facing the interaction point and proceeding clockwise, they are numbered 58, 59, 60, 01, 02...57 on the +z side and 118, 119, 120, 61, 62...117 on the -z side. Figure 14 shows the arrangement for the modules in the +z direction, while Figure 15 depicts the modules in the -z direction.



## EMC as seen from -z

Figure 15: EMC detector viewed from the outside while looking toward the interaction point.

Each EMC module has 40 towers. Each tower has a  $\phi$ -number (from 1-2) and a  $\eta$ -number (from 1-20). The  $\phi$ -towers are numbered from the perspective of an observer who is outside of the detector and looking at the EMC module. The towers are numbered clockwise with 1 as the first  $\phi$ -tower. Figure 16 shows a top view of the detector and illustrates the relationship between TPC sectors, EMC modules and EMC  $\phi$ -towers.

*View of the Detector from Above*  
 $-x$  (North)

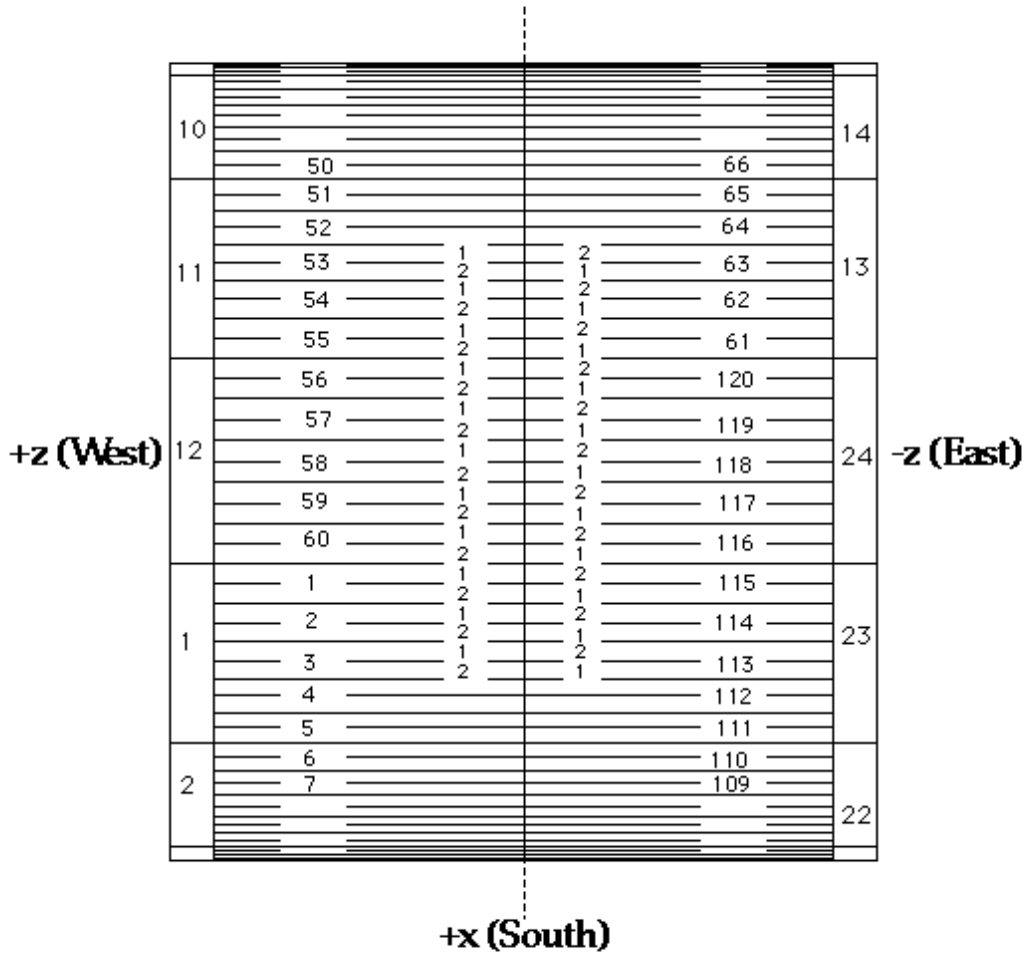


Figure 16: Top view of the detector. The numbers on the left and right edge show the TPC sector number. The numbers next to the TPC sectors are the EMC module numbers. The inner most numbers are the  $\phi$ -tower numbers.

Figure 17 shows the  $\eta$ -tower numbering. The upper section of the figure shows the top most tile layer. Towers of tiles are numbered from the center of the detector (starting with

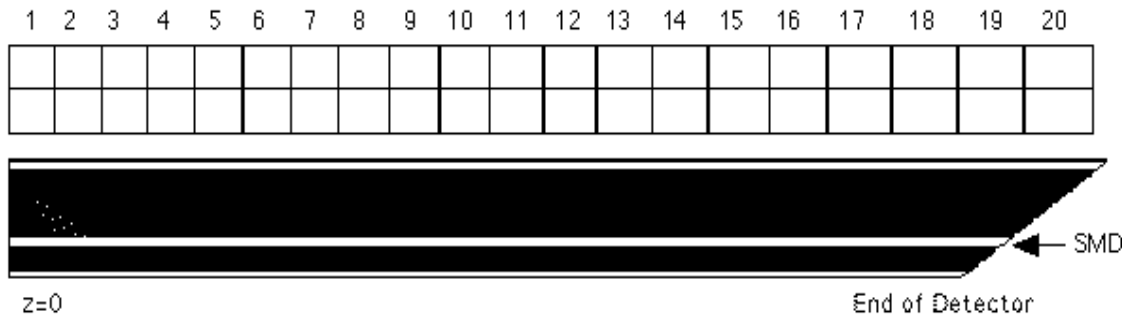


Figure 17: Schematic drawing of one STAR EMC modules showing a side view of the module and a top view of the last layer of tiles. The location of the Shower Max (SMD) is also shown. This view is for the  $-z$  side. The upper row of numbers is the  $\eta$ -tower number. The  $\eta$ -tower number on the  $+z$  side also starts numbering with 1 at  $z = 0$ .

1) to the outer edge (ending with 20). The figure also shows the  $\varphi$ -segmentation which was been discussed previously. The bottom section shows the location of the shower max. All EMC modules are numbered in  $z$  starting from the first  $\eta$ -tower at  $z = 0$ . Therefore, the  $\eta$ -tower at the end of the detector on both the  $+z$  and  $-z$  side ( $|\eta| = 1$ ) is #20.

Each EMC module contains one shower max detector (Figure 18), which has 300 strips. The shower max module is made of a front plane (closest to the interaction point), that has 2 patches of 75 strips each. From  $|\eta| < 0.5$ , there are 75 narrow strips which run perpendicular to the  $z$ -direction, numbering 1-75 starting from the middle of the detector ( $z=0$ ). For  $|\eta| > 0.5$ , there are 75 wide strips which run perpendicular to the  $z$ -direction, numbered 76-150, starting from  $|\eta| = 0.5$ , and numbered outwards from the center. The back plane layer is further from the interaction point, and has 10 patches, each of which covers  $\delta\eta$  of 0.1. There are 15 strips per patch, and they run in the  $\varphi$ -direction or parallel to the  $z$ -direction, they are numbered 1-15 clockwise (with respect to an observer facing the interaction point and outside the detector.)

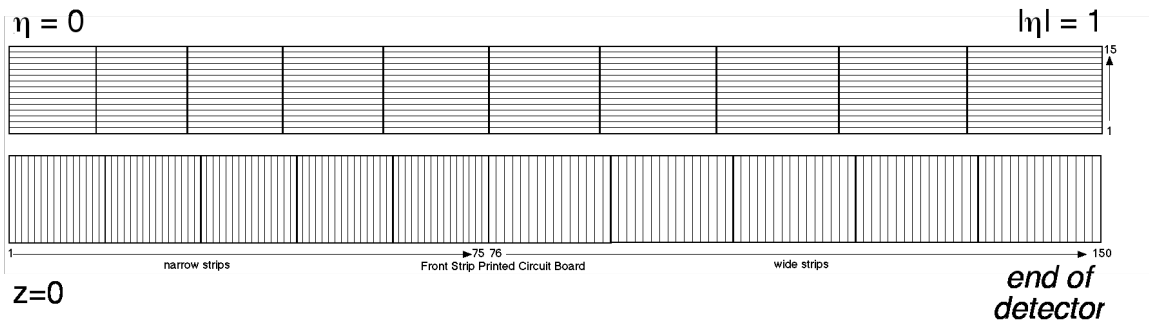
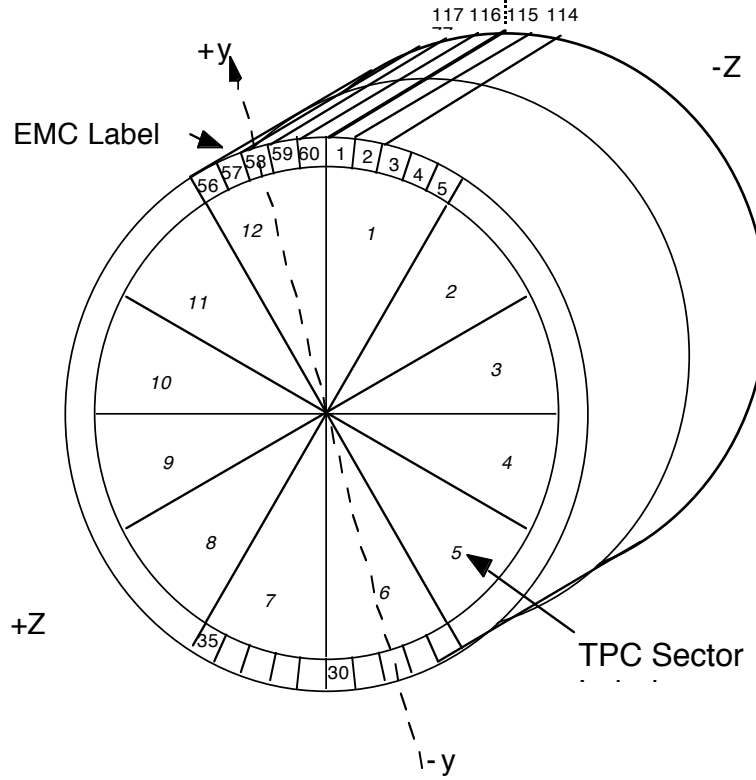


Figure 18: This figure shows the layout of the printed circuit. The top shows the  $\varphi$ -strips and bottom shows the  $\eta$ -strips. Note the two sizes of strips for the  $\eta$ -strips.

Another representation of the EMC detector can be found in Figure 19. The upper figure shows the relationship between the EMC modules on the  $+z$  and  $-z$  side. It shows how the modules are aligned with respect to the TPC detector. The lower figure describes the numbering for the  $\eta$ -strips and  $\varphi$ -strips.



### Three Dimension Layout of the EMC



### SHOWER MAX -- Top Radial View

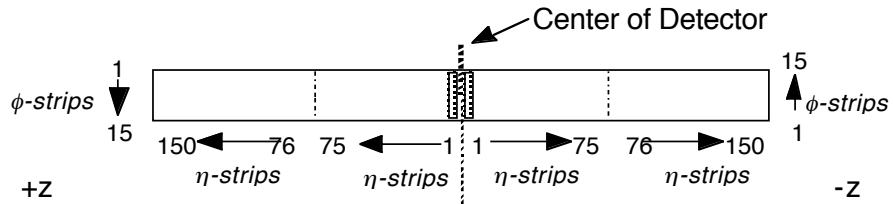


Figure 19: Relationship between the EMC modules on the +z and -z side. The labels for the shower max are also shown. The view on the shower max is from the perspective a person looking down from outside the detector.